CHEMPHYSCHEM

Torsional Barriers in Aromatic Molecular Clusters as Probe of the Electronic Properties of the Chromophore

Christoph Jacoby[b] and Michael Schmitt*[a]

We present a computer program that is capable of fitting n*-fold torsional barriers* V_n *(*n = *2–6) and torsional constants* F *simultaneously to high- and low-resolution spectroscopic data of different isotopomeric internal rotors. The program has been utilized to fit independently barriers and torsional constants for both electronic states of several aromatic clusters. The constant* F *of the ammonia moiety in the phenol–ammonia cluster is shown to decrease upon electronic excitation, thus imaging the formation of a hydrogen-bonded complex between the phenoxy radical and the* NH_4 *radical in the excited state. In contrast, for the naphthol–ammonia 1:1 clusters no change of* F *of ammonia could be found. For phenol–methanol cluster we found a decrease of* F *upon excitation which points to a stronger hydrogen bond between phenol and methanol in the excited state. A strong reduction of the torsional barrier upon excitation points to the formation of a methoxonium radical in a similar photoreaction as in phenol–ammonia cluster. For the phenol–water system we postulate the same mechanism, a photoreaction, which leads to a translocated hydrogen atom in the* S_1 *state what can be deduced from the change of the torsional constant upon electronic excitation.*

1. Introduction

The determination of torsional barriers and torsional constants in different electronic states of a molecule with an internal top attached to a rigid frame provides valuable insight into the electronic properties of the molecular frame. Spectroscopic information about torsional barriers is available from low-resolution experiments, resulting in torsional frequencies for the ground state by dispersed fluorescence (DF) spectroscopy and for the excited state (laser-induced fluorescence (LIF), resonance-enhanced two-photon ionization (R2PI) spectroscopy, etc.). The analysis of these data in terms of periodic potential functions has been described by Lewis et al.[1] High-resolution spectroscopy, that is, experiments with rotational or rovibronic spectral resolution, adds important information on the torsional perturbation term series. The corresponding theory has been developed by Lin and Swalen[2] and is used in a plethora of publications.

Most of the publications on internal rotor problems of three- or sixfold barriers are concerned with methyl tops. The use of the triply deuterated methyl top in spite of the normal isotopomer provides additional information on barriers and torsional constants in cases where not enough spectroscopic information is available from the methyl top. Use can be made of geometrical relations between the internal rotation constants of the different isotopomers. The torsional barrier is supposed to be the same for different isotopomers, what is strictly valid only in the Born–Oppenheimer approximation. Herein, we describe a computer program (HTorFit) which is capable of fitting torsional barriers and internal rotation constants to torsional frequencies and perturbation terms of several isotopic species of a (symmetric) top-attached to an asymmetric rigid frame.

Using the program we reanalyze the torsional structures of the hydrogen-bonded phenol–water, phenol–ammonia, and phenol–methanol clusters and compare them with results for the naphthol–ammonia clusters. As chromophore of the amino acid tyrosine, photoexcited clusters of phenol with different cluster partners found widespread interest as model systems for proton and electron transfer in excited states of amino acids. These processes play important roles in photobiology, for example, in the photosystem II. In the water-oxidizing complex of photosystem II, tyrosine is oxidized and reduced by electron–proton transfer and hydrogen atom transfer mechanisms involving tyrosine, water, and histidine.[3]

The phenol–water system shows a twofold periodic potential due to the internal rotation of the water moiety about the hydrogen bond while phenol–ammonia and phenol–methanol systems exhibit a threefold periodic potential due to the internal rotation of ammonia and of the methyl group, respectively. In these examples, interesting structural changes of the cluster occur when the chromophore (phenol) is excited to the S_1 state. They can be observed by the torsional potentials and torsional constants involved, which serve as a probe of the altered electronic and geometric surrounding of the cluster partner. As a general feature we found that in the first-excited sin-

[a] *Priv.-Doz. Dr. M. Schmitt*
Heinrich-Heine-Universität
Institut für Physikalische Chemie, 40225 Düsseldorf (Germany)
Fax: (+49) 211-81-15195
E-mail: mschmitt@uni-duesseldorf.de

[b] *Dr. C. Jacoby*
Heinrich-Heine-Universität
Institut für Herz- und Kreislaufphysiologie, 40225 Düsseldorf (Germany)

  DOI: 10.1002/cphc.200400281

glet state of all phenol clusters a H atom translocation to the respective cluster partner takes place. This mechanism was postulated for 1:1 clusters of the phenol–ammonia system to occur as hydrogen transfer after photoexcitation.[4] We propose the H translocation in the electronically excited S_1 state to be a more general photoreaction of phenol clusters, which is mostly independent of the nature of the cluster partner. In the cases studied here, an early stage of the formation of hydronium, ammonium, and methoxonium radicals due to H atom translocation from photoexcited phenol is postulated on the basis of different spectroscopic evidences. For the ammonia clusters of naphthol no such spectroscopic evidence is found.

2. Theory

2.1. The Pure Torsional Problem

In a one-dimensional model the torsional motion of an internal rotating symmetric top can be described by the Hamiltonian in Equation (1):

$$H_T = Fp^2 + \frac{1}{2}\sum_n V_n(1-\cos n\alpha) \quad (1)$$

with the angular momentum of the internal rotor defined by Equation (2)

$$p = -i\hbar\frac{d}{d\alpha} \quad (2)$$

and the torsional angle α. The kinetic energy term Fp^2 is that of a free rotor model with the torsional constant F, while the second term introduces a barrier consisting of different n-fold periodic potentials, where in our case n is restricted to a maximum value of six. Using the free rotor basis functions given in Equation (3):

$$|m\rangle = \frac{1}{\sqrt{2\pi}}e^{im\alpha} \quad m = 0, \pm 1, \pm 2, \ldots \quad (3)$$

one can set up the Hamiltonian matrix with the elements given in Equations (4a) and (4b),

$$\langle m|H_T|m\rangle = Fm^2 + \frac{1}{2}\sum_n V_n \quad (4a)$$

$$\langle m|H_T|m'\rangle = \langle m'|H_T|m\rangle = -\frac{1}{4}V_{|m-m'|} \quad \text{for } m \neq m' \quad (4b)$$

Diagonalization of this matrix provides the torsional energy levels as well as coefficients of the corresponding Eigenfunctions given in Equation (5),

$$\Psi_j = \frac{1}{\sqrt{2\pi}}\sum_{m=-\infty}^{\infty} A_m^{(j)}e^{im\alpha} \quad (5)$$

for the jth energy level. Two more quantum numbers, v and σ, are introduced to unambiguously classify the jth energy level in Equation (5). The principal torsional quantum number v is used to classify the torsional states for a single N-fold potential, and the N torsional sublevels have to be distinguished by a further quantum number σ. This σ is chosen in such a way that it represents the symmetry of the torsional wavefunctions and therefore, the torsional problem is diagonal in σ. The range of the integer σ is given by $-N/2 < \sigma \leq N/2$ and values only differing in sign build up a degenerate pair. For even v, the absolute value of σ increases with increasing energy, while the order is reversed for odd values of v.

For every electronic state, the torsional energy levels can be calculated from the respective set of parameters F and V_1–V_6. Transition energies between these states can easily be obtained relative to the difference of the vibronic ground states. In the program, a set of assigned transition energies can be fitted to the parameters of both vibronic states involved. If the internal rotating group is exchanged by an adequate isotopomeric group (e.g., CH_3 by CD_3), the barriers are assumed to be identical because of nearly identical electronic properties of these groups as long as the Born–Oppenheimer approximation holds. Hence, different energy values are assumed to result only from different values of F. Therefore, transitions from different isotopomers can be fitted synchronically to different values of F, where fixed relations between them can optionally be defined.

2.2. Coupling of Torsion and Overall Rotation

The one-dimensional model of a pure torsional motion has to be refined when high-resolution data (rotation) are taken into account. Due to coupling of torsion and overall rotation, the complete Hamiltonian is not separable into pure rotational and torsional parts. It can be written as Equation (6),

$$H = H_R + F(p-\mathfrak{P})^2 + \frac{1}{2}\sum_n V_n(1-\cos n\alpha) \quad (6)$$

where the first two terms describe the kinetic energies of overall and internal rotation, respectively, and the last term is the torsional potential energy as in Equation (1). In this form of the Hamiltonian, F (in Hz) is defined as Equation (7)

$$F = \frac{h}{8\pi^2 r I_\alpha} \quad (7)$$

with r given by Equation (8),

$$r = 1 - \sum_{g=a,b,c}\frac{\lambda_g^2 I_\alpha}{I_g} \quad (8)$$

where I_α is the moment of inertia of the internal rotor, the I_g are the principal moments of inertia of the whole molecule, and the λ_g are the direction cosines between the inertial axes and the axis of internal rotation. $\mathfrak{P}$ is defined by Equation (9)

$$\mathfrak{P} = \sum_{g=a,b,c}\rho_g P_g \quad (9)$$

with ρ_g given in Equation (10).

$$\rho_g = \lambda_g \frac{I_\alpha}{I_g} \tag{10}$$

The difference $p-\mathfrak{P}$ describes the angular momentum of the internal rotor relative to the frame. While the sum of Fp^2 and the potential energy term is identical to H_T in Equation (1), the quadratic term $F\mathfrak{P}^2$ can be absorbed into the rotational Hamiltonian H_R, which leads to slightly modified rotational constants, and so the Hamiltonian of Equation (6) can be rewritten as Equation (11).

$$H = H'_R + H_T - 2Fp\mathfrak{P} \tag{11}$$

In this equation the last term acts on the coordinates of overall and internal rotation, is nondiagonal in K and v, and can therefore not be solved without further approximations. By successive applications of a Van Vleck transformation[5] one can reduce the nondiagonal elements to any order. Generally, a reduction to second order is sufficient to neglect the remaining nondiagonal terms. In this way, the problem gets diagonal for the pure torsional part and we can solve the torsional and rotational problems separately in the usual way. This approximation is only valid, if the distances of the rotational levels are small compared to the levels of different v. Strictly, this condition is fulfilled only for high barriers, why it is called the high-barrier approximation. In some of the examples that we will give below, the barrier is low, on the order of 30–50 cm^{-1}. Nevertheless, the torsional energy splitting is larger by at least an order of magnitude compared to the rotational level separation. Thus, also in these cases the approximation for the high-barrier limit holds.

The resulting Hamiltonian of the torsion–rotation interaction given by $-2Fp\mathfrak{P}$, which is correct up to second order in the high-barrier limit, can be written as Equation (12),[6,7]

$$H_{RT}^{v\sigma} = FW_{v\sigma}^{(1)} \sum_{g=a,b,c} \rho_g P_g + FW_{v\sigma}^{(2)} \sum_{g=a,b,c} (\rho_g P_g)^2 \tag{12}$$

where the $W_{v\sigma}^{(n)}$ are the perturbation coefficients to the order n. The Van Vleck transformation leads to two modifications in the rotational Hamiltonian $H_R^{v\sigma}$, which is only valid for one specific torsional state $|v,\sigma\rangle$. The quadratic terms in Equation (12) can be incorporated into the rotational constants of the pure rotational Hamiltonian. For a threefold potential, for example, there are two different sets of rotational constants $B_g^{v,0}$ and $B_g^{v,\pm1}$ for every v. The geometrical rotational constants B_g can easily be determined from these quantities (see Equation (16), below). The second modification is the introduction of terms that are linear in the components of angular momentum and are only nonzero for degenerate levels. The resulting effective rotational Hamiltonian for the state $|v,\sigma\rangle$ can now be written as Equation (13),

$$H_R^{v\sigma} = \sum_{g=a,b,c} B_g^{v\sigma} P_g^2 + \sum_{g=a,b,c} D_g P_g \tag{13}$$

where the D_g are defined by Equation (14).

$$D_g = \rho_g F W_{v\sigma}^{(1)} = \frac{\lambda_g B_g W_{v\sigma}^{(1)}}{r} \tag{14}$$

Here, $W_{v\sigma}^{(1)}$ is the first-order perturbation coefficient for the state $|v,\sigma\rangle$ coming from the Van Vleck transformation and it is given by Equation (15).

$$W_{v\sigma}^{(1)} = -2\langle v\sigma|p|v\sigma\rangle \tag{15}$$

The $B_g^{v\sigma}$ are defined by Equation (16)

$$B_g^{v\sigma} = B_g + FW_{v\sigma}^{(2)}\rho_g^2 \tag{16}$$

with second-order perturbation coefficients $W_{v\sigma}^{(2)}$ given by Equation (17).

$$W_{v\sigma}^{(2)} = 1 + 4F \sum_{v'\neq v} \frac{|\langle v\sigma|p|v'\sigma\rangle|^2}{E_{v\sigma} - E_{v'\sigma}} \tag{17}$$

The integrals which are used to calculate the perturbation coefficients in Equation (15) and Equation (17) can easily be determined from the coefficients of the torsional Eigenfunctions given in Equation (18).

$$\langle v\sigma|p|v'\sigma\rangle = \sum_{m=-\infty}^{\infty} mA_m^{v\sigma} A_m^{v'\sigma} \tag{18}$$

2.3. Program Options

We set up the HTorFit program for a simultaneous fit of the reduced barrier height in both electronic states to the experimentally determined torsional splitting $E_{v,0}-E_{v,\pm1}$ from solving Equation (1), to the difference of the rotational constants $\Delta B_g = B_g^{v,0} - B_g^{v,\pm1}$ [see Equation (16)], and to the torsion–rotation parameters D_g [Equation (14)] of several isotopomers using the Levenberg–Marquardt algorithm as local minimizer.[8,9] Also D_g and ΔB_g parameters for higher v states can be fitted. Furthermore, the program is capable of fitting the barriers and torsional constants of both electronic states to torsional transitions of different v in absorption $E_{v'\sigma} \leftarrow E_{v''\sigma}$ or in emission $E_{v'\sigma} \rightarrow E_{v''\sigma}$. They are obtained from low-resolution spectra of several isotopomers. The transitions may be defined in $v\sigma$ or $m\sigma$ nomenclature in the input file, where the classification m refers to the quantum numbers of the free rotor basis functions, defined in Equation (3). While the $v\sigma$ nomenclature is used in the case of twofold barriers, the $m\sigma$ nomenclature is more frequently utilized for threefold potentials. Anyhow, both can be used to assign transitions for all types of barriers in the program.

Barriers and torsional constants can be fitted in one electronic state and confined to the fitted value in the other electronic state or they may be fitted independently in both states. Relations between the torsional constants of the isotopomeric tops can be used, for example, $F(CH_3) = 2 \cdot F(CD_3)$ or they may be fitted independently. Potential barriers are assumed to be equal for different isotopomeric tops attached to identical frames what is valid in the Born–Oppenheimer approximation.

The standard deviations of the fit parameters are determined from the covariance matrix using the uncertainties of the experimental values.

3. Results and Discussion

As examples for possible applications of our program, we chose molecular systems with two- and threefold barriers, but there is no limitation to these cases. The change of F upon electronic excitation bears important information about structural changes of the top. Nevertheless, in many cases it is not possible to fit F of both states independently of the barriers, which is due to a lack of sufficient spectroscopic data. This lack sometimes impedes the independent fit of both F values, that is, the ground and excited state F have to be set equal. We will show in the following how the program can be utilized to combine all spectroscopic information about the barriers and the torsional constants in two different states from several isotopomeric tops.

3.1. Threefold Barriers

Threefold barriers are probably the most abundant case of all hindering potentials. A large number of molecules has been investigated by using both high- and low-resolution spectroscopy. We tested our program on a number of molecules with threefold rotors, among them 1- and 2-methylnaphtalene,[10] 1-methylindole,[11,12] 3-methylindole,[13,14] and 5-methylindole[11,13,14] and found good agreement with the cited barriers and internal rotation constants in all cases. As the geometry change along the torsional coordinate upon electronic excitation is small, the torsional transitions in these molecules are generally weak. Therefore, in many cases not enough spectroscopic information provided for an independent fit of the torsional constants in both states. This is true especially for cases in which the internal rotation takes place not in the chromophore itself, but in a second molecule which is hydrogen- or van der Waals-bound to the chromophore. In these cases, the use of additional spectroscopic information from isotopomeric species adds valuable information for the independent determination of barriers and torsional constants in both electronic states.

The method is applied to clusters of ammonia and methanol with naphthol isomers and phenol. The geometry change of the top in these clusters can be utilized as a probe for the different electronic properties of the chromophore upon excitation. We will show in the following, how an independent evaluation of the torsional constants in both electronic states permits interpretation of exited state photoreactions between the chromophore and the cluster partner. The structures of the molecules discussed herein and the orientation of the torsional axes are shown in Scheme 1.

Trans-*1-Naphthol(NH_3)$_1$*

Torsional bands of *trans*-1-naphthol(NH_3)$_1$ have been observed for the ground and excited state by using DF and R2PI spectroscopy, respectively.[15] Furthermore, excited-state torsional bands were given in the above publication for the [d_3]1-naphthol(ND_3)$_1$ tautomer. Humphrey and Pratt[16] presented the rotationally resolved spectrum of the electronic origin of 1-naphthol(NH_3)$_1$. From their experiments the *AE* splitting and the torsion–rotation perturbation terms $D_{a,b}$ in both electronic states were determined. Table 1 summarizes the experimental data and the results of a fit with our program HTorFit, using the approximation of $F(NH_3) = 2F(ND_3)$.

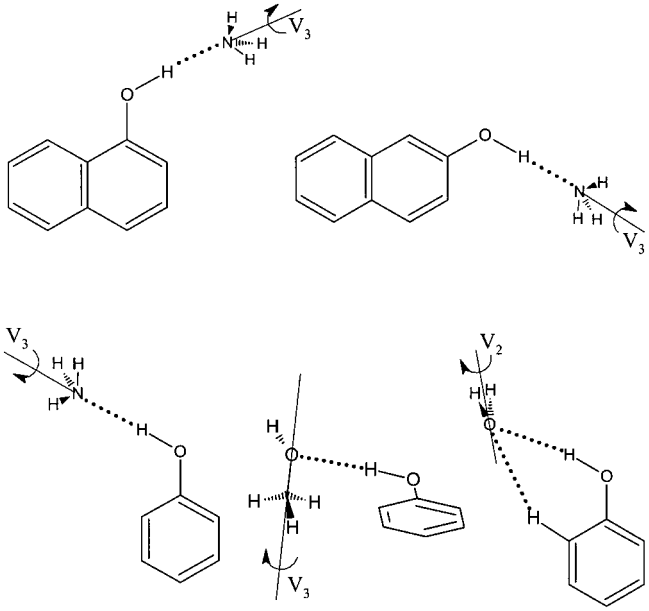

Scheme 1. *Structures of the 1-naphthol–ammonia, 2-naphthol–ammonia, phenol–ammonia, phenol–methanol and phenol–water clusters along with the orientation of the respective torsional axis.*

In this way it was possible to fit the ground- and excited-state V_3 barriers and the torsional constants in both states independently. The fit resulted in barriers of $V_3'' = 40.2\ cm^{-1}$ and $V_3' = 46.8\ cm^{-1}$, respectively. F was determined to be nearly the same in both electronic states ($6.71\ cm^{-1}$). These values are close to the values determined by Humphrey and Pratt[16] who made the assumption that the torsional constants are equal in both electronic states ($F = 6.62\ cm^{-1}$, $V_3'' = 39.9\ cm^{-1}$, $V_3' = 46.5\ cm^{-1}$).

Trans-*2-Naphthol(NH_3)$_1$*

Torsional bands of *trans*-1-naphthol(NH_3)$_1$ have been observed for the ground and excited state by using DF and R2PI spectroscopy, respectively.[17] A vibronic band at $33.5\ cm^{-1}$ was assigned to the intermolecular β_1 vibration and a transition at $27\ cm^{-1}$ in the DF spectrum to the same transition in the ground state.[17] On the basis of the fit to the torsional spectrum, we propose another assignment of these two bands. Both fit perfectly to the $2e \leftarrow 1e$ ($33.5\ cm^{-1}$) and $1e \rightarrow 2e$ ($-27\ cm^{-1}$) transitions, respectively. Plusquellic et al. determined the torsion–rotation perturbation terms and the *AE* splitting from the rotationally resolved spectrum of the electronic origin of *trans*-1-naphthol(NH_3)$_1$.[18] As in the case of

Table 1. *Torsional parameters of the hydrogen-bonded* trans*-1-naphthol$(NH_3)_1$ cluster. The electronic transitions are labeled by the* m *quantum number and the symmetry of the subtorsional level* σ*:* mσ*(S_1)←*mσ*(S_0) for absorption bands and* mσ*(S_1)→*mσ*(S_0) for emission bands.* $\Delta B_g = B_g^{v,0} - B_g^{v,\pm 1}$ *for* v = *0.* F *is identical to* $F(NH_3) = 2F(ND_3)$.

	Exptl.	Fit.	Exptl−Fit	Unit
trans-1-naphthol$(NH_3)_1$				
$1e \leftarrow 1e$	−0.429(2)[a]	−0.429	0	cm^{-1}
$2e \leftarrow 1e$	29.2(2)[b]	30.3	−1.1	cm^{-1}
$3a_1 \leftarrow 0a_1$	70.6(2)[b]	67.8	−2.8	cm^{-1}
$0a_1 \rightarrow 3a_1$	−69(5)[c]	−66	−3	cm^{-1}
$D_a(S_0)$	2001.3(2)[a]	2001.3	0	MHz
$D_b(S_0)$	0(25)[a]	0	0	MHz
$D_a(S_1)$	1745.0(2)[a]	1745.0	0	MHz
$D_b(S_1)$	0(25)[a]	0	0	MHz
$\Delta B_a(S_0)$	12.2(2)[a]	12.6	−0.4	MHz
$\Delta B_b(S_0)$	−0.1(2)[a]	0.0	0	MHz
$\Delta B_a(S_1)$	12.4(2)[a]	12.9	−0.5	MHz
$\Delta B_b(S_1)$	0.0(1)[a]	0.0	0	MHz
[d_3]*trans*-1-naphthol$(ND_3)_1$				
$2e \leftarrow 1e$	26.0(2)[b]	26.4	−0.4	cm^{-1}
$3a_1 \leftarrow 1a_1$	40.5(2)[b]	45.5	−5.0	cm^{-1}
$4e \leftarrow 1e$	61.5(2)[b]	60.0	1.5	cm^{-1}
$V_3(S_0)$		40.15(20)		cm^{-1}
$F(S_0)$		6.712(34)		cm^{-1}
$V_3(S_1)$		46.79(25)		cm^{-1}
$F(S_1)$		6.716(37)		cm^{-1}

[a] *AE* splitting, ΔB_g, and D_g constants from Humphrey et al.[16] [b] Vibronic transitions from Henseler et al.[15] [c] DF data from Henseler et al.[15]

trans-1-naphthol$(NH_3)_1$, the fit resulted in almost equal torsional constants for the ground and excited state (6.59 cm^{-1}). Barriers of $V_3'' = 33.9\ cm^{-1}$ and $V_3' = 57.9\ cm^{-1}$ were obtained (Table 2).

Table 2. *Torsional parameters of* trans*-2-naphthol$(NH_3)_1$. The electronic transitions are labeled by their* m *and* σ *quantum numbers:* mσ*(S_1)←*mσ*(S_0) for absorption bands and* mσ*(S_1)→*mσ*(S_0) for emission bands.* $\Delta B_g = B_g^{v,0} - B_g^{v,\pm 1}$ *for* v = *0.*

	Exptl.	Fit	Exptl.−Fit	Unit
trans-2-naphthol$(NH_3)_1$				
$1e \leftarrow 1e$	−45439.8(2)[a]	−45439.8	0	MHz
$2e \leftarrow 1e$	33.5(1)[b]	33.5	0	cm^{-1}
$1e \rightarrow 2e$	−27.4(10)[c]	−27.7	−0.3	cm^{-1}
$D_a(S_0)$	3274.7(1)[a]	3274.7	0	MHz
$D_b(S_0)$	233.9(1)[a]	233.9	0	MHz
$D_a(S_1)$	1911.8(1)[a]	1911.8	0	MHz
$D_b(S_1)$	174.9(1)[a]	174.9	0	MHz
$\Delta B_a(S_0)$	27.6(3)[a]	25.7	1.9	
$\Delta B_b(S_0)$	0.0(2)[a]	0.1	−0.1	
$\Delta B_a(S_1)$	26.4(3)[a]	24.6	1.8	
$\Delta B_b(S_1)$	0.0(2)[a]	0.2	−0.2	
$V_3(S_0)$		33.79(68)		cm^{-1}
$F(S_0)$		6.586(13)		cm^{-1}
$V_3(S_1)$		57.829(165)		cm^{-1}
$F(S_1)$		6.593(19)		cm^{-1}

[a] *AE* splitting, ΔB_g, and D_g constants from Plusquellic et al.[18] [b] Vibronic transitions from Droz et al.[17] [c] DF data from Droz et al.[17]

The change in barrier height upon electronic excitation is slightly different from the respective values determined by Plusquellic et al.[18] by using the approximation of equal F for both electronic states ($F = 6.58\ cm^{-1}$, $V_3'' = 34.2\ cm^{-1}$, $V_3' = 58.2\ cm^{-1}$).

Thus, for both naphthol–ammonia clusters the torsional constant and therefore the geometry of the ammonia moiety does not change upon electronic excitation. We will show in the following that this is different for clusters of phenol.

Phenol$(NH_3)_1$

The vibronic spectrum of the hydrogen-bonded phenol$(NH_3)_1$ cluster has been observed by using two-color R2PI spectroscopy.[19] Due to unfavorable Franck–Condon factors, only one torsional band in the electronically excited state could be assigned. Jacoby[20] investigated the vibronic spectrum of the phenol$(ND_3)_1$ cluster and found three bands which can be assigned to torsional transitions of the ND_3 moiety. By using these four transitions, one from phenol$(NH_3)_1$ and three from phenol$(ND_3)_1$, the V_3 barriers and the torsional constants of both electronic states could be calculated. On the basis of this calculation, we performed a simulation with $V_3'' = 34.1\ cm^{-1}$, $F'' = 6.656\ cm^{-1}$, $V_3' = 54.5\ cm^{-1}$, and $F_3' = 5.978\ cm^{-1}$, which allowed us to assign two more torsional transitions in the normal isotopomer. They appear in the R2PI spectrum of ref. [19], but they are very weak in the hole-burning spectrum shown in the same publication. For that reason, they were classified as bands from fragmentation of higher clusters. From the simulation, we predict these two bands to be the $2e \leftarrow 1e$ and the $4e \leftarrow 1e$ torsional transitions (Table 3).

Table 3. *Torsional parameters of phenol$(NH_3)_1$. The electronic transitions are labeled by their* m *and* σ *quantum numbers:* mσ*(S_1)←*mσ*(S_0).*

	Exptl.	Fit	Exptl.−Fit	Unit
phenol$(NH_3)_1$				
$2e \leftarrow 1e$	31.0(2)[a]	31.3	−0.3	cm^{-1}
$3a_1 \leftarrow 0a_1$	64.5(2)[a]	65.2	0.3	cm^{-1}
$4e \leftarrow 1e$	99.0(2)[a]	98.7	0.3	cm^{-1}
phenol$(ND_3)_1$				
$2e \leftarrow 1e$	26.9(2)[b]	26.9	0.0	cm^{-1}
$3a_1 \leftarrow 0a_1$	45.9(2)[b]	45.3	0.6	cm^{-1}
$4e \leftarrow 1e$	59.2(2)[b]	59.5	−0.3	cm^{-1}
$V_3(S_0)$		34.1(20)		cm^{-1}
$F(S_0)$		6.656(121)		cm^{-1}
$V_3(S_1)$		54.5(3)		cm^{-1}
$F(S_1)$		5.978(19)		cm^{-1}

[a] Vibronic bands of phenol$(NH_3)_1$ from Schiefke et al.[19] [b] Vibronic bands of phenol$(ND_3)_1$ from Jacoby.[20]

By using the barriers and torsional constants quoted above a subtorsional splitting of 1.5 cm^{-1} is predicted for the electronic origin. If the hole-burning spectrum shown in ref. [19] was analyzed at the high-frequency side of the origin band,

the small intensity of the E bands in the hole-burning spectrum could easily be explained.

In contrast to the naphthol$(NH_3)_1$ clusters, the torsional constant of phenol$(NH_3)_1$ changed considerably upon electronic excitation. The phenol–ammonia cluster shows in some respect a quite different behavior compared to that of other hydroxyaromatics–ammonia clusters. The lifetimes of *trans*-1-naphthol$(NH_3)_1$ and *trans*-2-naphthol$(NH_3)_1$ have been determined to be 40 ns and 31 ns, respectively,[16,18] while the lifetime of phenol$(NH_3)_1$ is only about 1 ns.[4] This short lifetime has been attributed to the excited-state photoreaction, Equation (19),

$$PhOH^*-NH_3 \rightarrow PhO^{\cdot} \cdots NH_4^{\cdot} \quad (19)$$

by Grégoire et al.[4,21] The rotational constant of ammonia about its symmetry axis is 6.228 cm^{-1},[22] while the rotational constant of the spherical rotor $NH_4^{\cdot}$ is 5.674 cm^{-1}, determined from a rotationally resolved photoelectron spectrum.[23] This difference between the rotational constants of NH_3 and $NH_4^{\cdot}$ is similar to the reduction of *F*, which we observe in the phenol–ammonia cluster upon electronic excitation. Therefore, we propose that the torsional constants image the change of the geometry in the electronically excited $^1\pi\pi^*$ state of phenol$(NH_3)_1$ due to an early precursor of the excited-state photoreaction [Equation (19)] leading to the Rydberg radical $NH_4^{\cdot}$. CASSCF calculations of Domcke and Sobolewski show, that the vertically excited $^1\pi\pi^*$ state has a structure in which the phenoxy radical is hydrogen-bonded to the $NH_4^{\cdot}$ radical.[24] In this picture, the H atom transfer could be viewed as a transition from the directly excited $^1\pi\pi^*$ state to the $^1\pi\sigma^*$ state with a low barrier separating them.

Table 4 shows the result of the fit. If both torsional constants and the barriers in both electronic states are fitted independently, we obtain a value for *F*, which cannot be interpreted geometrically. On the other hand, the experimentally determined parameters could not be fitted by assuming equal *F* for both states, or for torsional constants, which are close to a geometrically meaningful value of around 5 cm^{-1}.

Table 4. *Torsional parameters of phenol–methanol cluters. The electronic transitions are labeled by their* m *and* σ *quantum numbers:* $m\sigma(S_1) \leftarrow m\sigma(S_0)$ *for absorption bands.*

	Exptl.	Fit	Exptl.−Fit	Unit
phenol$(CH_3OH)_1$				
$1e \leftarrow 1e$	3557.621(740)[a]	3557.621	0	
$D_a(S_0)$	32.83(34)[a]	32.85	−0.2	MHz
$D_b(S_0)$	14.3(78)[a]	14.3	0	MHz
$D_c(S_0)$	40.312(178)[a]	40.332	−0.2	MHz
$D_a(S_1)$	78.90(32)[a]	79.5	−0.6	MHz
$D_b(S_1)$	38.2(34)[a]	38.5	−0.3	MHz
$D_c(S_1)$	52.134(187)[a]	52.532	−0.398	MHz
phenol$(CD_3OH)_1$				
$1e \leftarrow 1e$	438.52(107)[b]	438.52	0	MHz
$D_a(S_0)$	3.188(100)[c]	3.307	0.119	MHz
$D_b(S_0)$	1.497(100)[c]	1.553	−0.056	MHz
$D_c(S_0)$	2.722(100)[c]	2.823	−0.101	MHz
$D_a(S_1)$	11.124(400)[c]	10.241	0.883	MHz
$D_b(S_1)$	4.348(400)[c]	4.003	0.345	MHz
$D_c(S_1)$	5.667(400)[c]	5.217	0.450	MHz
$V_3(S_0)$		520.2(39)		cm^{-1}
$F(S_0)$		16.193(130)		cm^{-1}
$V_3(S_1)$		328.7(38)		cm^{-1}
$F(S_1)$		11.972(130)		cm^{-1}

[a] *AE* splitting and D_g constants from Schmitt et al.[26] [b] *AE* splitting from Westphal et al.[27] [c] D_g constants from ref. [30].

Phenol$(CH_3OH)_1$

The phenol–methanol cluster presents an interesting example of an internal rotation in which the top is not directly attached to the chromophore through a hydrogen bond such as in phenol–ammonia clusters. Furthermore, three projections of the internal rotor axes have to be taken into account in contrast to the above examples of a top-attached to a planar frame. No torsional bands can be observed in the low-resolution spectra because of unfavorable Franck–Condon factors, but the torsional splitting between $0a_1 \leftarrow 0a_1$ and $1e \leftarrow 1e$ was observed in combination with all vibronic bands. Symmetry-labeled hole-burning spectroscopy has been performed, but no bands were found because of pure excitation of the torsional motion.[25] The perturbation terms and *AE* splitting for phenol-(CH_3OH) are taken from ref. [26], those for phenol(CD_3OH) from Westphal et al.[27] The perturbation terms for phenol(CD_3OH) from ref. [27] contain large uncertainties which is due to a small number or completely resolved rovibronic lines. We performed a global fit to the lineshape of the complete transition using a genetic algorithm (GA) based fitting scheme.[28,29] In this fit, all transitions are accounted for and much more accurate values for the D_g are obtained.[30]

It is well known for the methanol dimer, that the internal rotation of the methyl group is strongly perturbed by the librational motion of the acceptor moiety about the *a* axis of methanol.[31] Axes and displacement vectors for both motions nearly coincide as has been shown for the phenol–methanol cluster as well.[25] Thus, a strong coupling of both motions is plausible.

The barrier to methyl torsion in free methanol from microwave spectroscopy is 376.8 cm^{-1}.[32] The internal rotation constant *F* in the methanol monomer is determined to be 27.634 cm^{-1}.[33] For a very weak (hydrogen) bond between the two moieties the value of *F* should approach this value of free methanol, while the other limit for a strongly bound methanol would be about 5.2 cm^{-1}, calculated from the geometrical I_α of the methyl group attached to a heavy frame. Our analysis gives an intermediate value of 16.2 cm^{-1} for the electronic ground state and of 12.0 cm^{-1} for the electronically excited state. These values reflect the increased hydrogen-bond strength in the electronically excited state of phenol–methanol cluster.

Assuming hydrogen atom translocation from photoexcited phenol to the methanol moiety, we are able to explain the large decrease of barrier height upon electronic excitation. The

torsional barrier of methanol, the methoxonium cation ($CH_3OH_2^+$) and the methoxonium radical ($CH_3OH_2^{\bullet}$) have been calculated at the UMP2/6-311G(d,p) level of theory. Although the absolute torsional barrier cannot be reproduced with high accuracy, the relative changes between the barriers of the three species are sufficiently exact in order to explain the observed differences. Figure 1 depicts the results of the calculations. The torsional barrier of methanol is overestimated at this level of theory (506 cm^{-1}). The barrier of the methoxonium cation is found to be even slightly larger (530 cm^{-1}) than the methanol barrier. The barrier of the methoxonium radical shows exactly the effect that is observed in the experiment: a distinct reduction in barrier height compared to that of methanol (399 cm^{-1}), see Table 4.

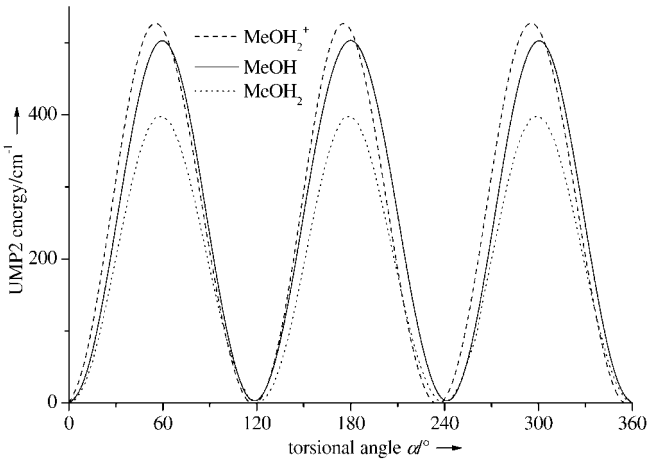

Figure 1. *MP2/6-311G(d,p) ab initio torsional potentials of methanol (solid line ——), the methoxonium cation (dashed line -----), and the methoxonium radical (dotted line •••••). Zero degrees refer to the most-stable staggered conformation of methanol (S), 60 degrees to the eclipsed conformer (E).*

Thus, we propose a photoreaction that is equivalent to phenol–ammonia clusters to take place in phenol–methanol clusters with the phenolic H atom translocated from the phenol to the methanol moiety [see Eq. (20)].

$$PhOH^*-CH_3OH \rightarrow PhO^{\cdot} \cdots CH_3OH_2^{\cdot} \qquad (20)$$

3.2. Twofold Barriers

In the principal-axis method (PAM)[6] used herein, the principal axes of the entire molecule are considered as reference system for the rotation of the top. A symmetric top ($n \geq 3$) leaves this reference system unaltered during rotation, while an asymmetric top changes the orientation of the inertial axes, thus violating the preconditions for the PAM. If, on the other hand, the asymmetric top is sufficiently light compared to the frame, the orientation of the top axis remains nearly unaltered by the torsion. This condition is fulfilled for the torsion of the water moiety in the phenol–water cluster ($n = 2$). We will discuss this system in the following.

Phenol(H_2O)$_1$

The subtorsional splitting between the transitions ($\sigma = 0)' \leftarrow (\sigma = 0)''$ and $(\sigma = 1)' \leftarrow (\sigma = 1)''$ was determined to be 25 455(10) MHz by Berden et al. by using rotationally resolved UV spectroscopy.[34] No information on the first-order perturbation coefficients is available from a twofold potential because of the lack of degenerate levels in this case. The second-order perturbation coefficients can be obtained from the difference of the rotational constants of ($\sigma = 0$) and ($\sigma = 1$) levels. Furthermore, the torsional bands in the electronically excited state obtained by R2PI and UV–UV double resonance spectroscopy[35] and in the ground state obtained by DF spectroscopy[36] were utilized in the fit. Due to unfavorable Franck–Condon factors, only few torsional bands can be observed, so that additional information from different isotopomers has to be used. We included the torsional bands of phenol(D_2O)$_1$ in the fit using the approximate relations between the torsional constants, $F(H_2O) = 2F(D_2O)$. The results of the fit are shown in Table 5.

Table 5. *Torsional parameters of two isotopomeric phenol–water clusters. The transitions are labeled by $|v\sigma\rangle' \leftarrow |v\sigma\rangle''$ for absorption and $|v\sigma\rangle' \rightarrow |v\sigma\rangle''$ for emission lines. $\Delta B_g = B_g^{v,0} - B_g^{v,1}$ for $v = 0$.*

	Exptl.	Fit	Exptl.−Fit	Unit
phenol(H_2O)$_1$				
$\|0,1\rangle' \leftarrow \|0,1\rangle''$	25455(10)	25454	1	MHz
$\|2,0\rangle' \leftarrow \|0,0\rangle''$	94.3(5)	93.7	0.6	cm^{-1}
$\|2,1\rangle' \leftarrow \|0,1\rangle''$	153.0(5)[b]	153.6	0.6	cm^{-1}
$\|2,0\rangle' \leftarrow \|0,0\rangle''$	−126(1)	−127	−1	cm^{-1}
$\Delta B_a(S_0)$	−9.73(5)[a]	−9.76	0.3	MHz
$\Delta B_b(S_0)$	0.181(3)[a]	0	0.181	MHz
$\Delta B_c(S_0)$	0.181(3)[a]	0	0.181	MHz
$\Delta B_a(S_1)$	−21.40(160)[a]	−20.97	0.43	MHz
$\Delta B_b(S_1)$	0.03(40)[a]	0	0.03	MHz
$\Delta B_c(S_1)$	0.23(16)[a]	0	0.230	MHz
phenol(D_2O)$_1$				
$\|0,1\rangle' \leftarrow \|0,1\rangle''$	0.1(1)[b]	0.121	0	cm^{-1}
$\|2,0\rangle' \leftarrow \|0,0\rangle''$	77.9(5)[b]	76.4	1.3	cm^{-1}
$\|4,0\rangle' \leftarrow \|0,0\rangle''$	150.3[b]	150.6	-0.3	cm^{-1}
$V_2(S_0)$		175.4(13)		cm^{-1}
$F(S_0)$		14.813(118)		cm^{-1}
$V_2(S_1)$		109.1(2)		cm^{-1}
$F(S_1)$		13.415(25)		cm^{-1}

[a] Experimental torsional splitting and ΔB_g from Berden et al.[34] [b] Torsional bands from Schmitt et al.[35] [c] DF from ref. [36].

The torsional constants could be determined independently for both electronic states. The fit yields $F'' = 14.813\ cm^{-1}$ and $F' = 13.415\ cm^{-1}$, showing a decrease of F upon electronic excitation. This reduction of F might be explained by the same photoreaction mechanism as in phenol–ammonia and phenol–methanol clusters. A hydrogen atom translocation takes place in the S_1 state from the phenol to the water moiety.

The rotational constant of water for rotation about the symmetry axis is 14.51 cm^{-1},[37] while the corresponding (calculated) rotational constant of $H_3O^{\bullet}$ is 9.85 cm^{-1}.[38] The torsional constant of the ground state differs slightly from the B rota-

tional constant of water indicating that the internal rotation is not a simple one-dimensional rotation about the symmetry axis of the water moiety. Instead, it is a more complicated motion, which couples the torsional motion and the in-plane bending motion of the water moiety.[34,39,40] A complete six-dimensional analysis of the intermolecular vibrations of phenol–water clusters by Jansen and Gerhards[41] shows that indeed all six intermolecular vibrations are strongly coupled, giving further evidence that a one-dimensional analysis of the torsion might not be appropriate in the case of this cluster. Therefore, the torsional constant is not conserved during the torsional motion, and the discussion of relative changes upon electronic excitation is more speculative than in the above cases.

This interpretation is supported by IR measurements of the phenolic OH stretching frequency in the S_1 state of the phenol–water cluster.[42] A larger redshift of the OH stretching frequency in the S_1 state compared to that of the S_0 state points to a considerable attraction of the H atom to the water site in agreement with the above considerations. On the other hand the antisymmetric OH stretch vibration of the water moiety does not change upon electronic excitation.[43] If the H atom was dislocated considerably, this frequency should also decrease by a large amount.

The V_2 barriers in ground and excited states are determined to be 175.4 cm^{-1} and 109.1 cm^{-1}, respectively. As the O···O distance between phenol and water decreases upon electronic excitation, one should expect an increase of the torsional barrier because of increased sterical hindrance. Nonetheless, the opposite is observed experimentally. In the *trans*-linear structure of the hydrogen-bonded phenol–water cluster, the OH···O distance of the hydrogen bond is calculated at the MP2/6-31G(d,p) level of theory to be 185.8 pm.[44] The CH···O distance of the *ortho*-CH group in phenol is calculated at the same level to be 270.2 pm. Thus, two hydrogen bonds are formed, a stronger OH···O and a weaker CH···O bond, see Scheme 1. If we look to the localized molecular orbitals, both hydrogen bonds are oriented in the direction of the equivalent oxygen lone pairs of the water moiety, thus hindering efficiently the torsional motion. When the phenolic H atom is translocated towards the water moiety, its structure will become nonplanar and the remaining lone pair will be less directed in direction of the *ortho*-CH bond. This fact might explain the surprising decrease of the torsional barrier upon electronic excitation.

4. Conclusions and Outlook

Torsional barriers and torsional constants of hydrogen-bonded clusters of phenol with ammonia, methanol, and water have been determined from various experimental findings. In all three cases, changes of the torsional constants and barriers are observed, which suggest a hydrogen atom translocation to occur in the electronically excited state of the cluster. For comparison to the phenol case, we also investigated the ammonia clusters of *trans*-1- and *trans*-2-naphthol. In these clusters, the torsional constant is determined to be the same in both electronic states. Therefore, no geometry change of the ammonia moiety is observed. In contrast, the value of *F* in the phenol–ammonia cluster decreases by almost 10% upon excitation. Such a large decrease denotes a considerable change of the structure of the ammonia top. It might be explained by an increased NH bond length or/and by an increased H–N–H bond angle. We trace the decrease of *F* back to an H atom transfer in the excited state, which forms the ammonium Rydberg radical. This mechanism has been proposed by Gregoire et al.[4,21] based on the lifetimes of several phenol–ammonia clusters and their perdeuterated isotopomers.

While the torsional motion in phenol–ammonia takes place about the hydrogen bond ("intermolecular torsion"), it is located in the methanol moiety of the phenol–methanol cluster ("intramolecular torsion"). Two effects have to be discussed for the phenol–methanol cluster. A strong coupling between the torsion and an in-plane librational motion leads to values of *F* which cannot be interpreted geometrically. The value of *F* should lie between the limits of a methyl top in the cluster (5.2 cm^{-1}) and in the pure methanol (27.6 cm^{-1}). The weaker the hydrogen bond between the cluster partners, the closer the value should approach the value of *F* for pure methanol. In our analysis, we found a decrease of *F* from 16.2 cm^{-1} to 12.0 cm^{-1} upon electronic excitation, which reflects the increased hydrogen bond strength in the S_1 state. The other effect which has to be explained is the large decrease of barrier height upon electronic excitation (from 520 cm^{-1} to 329 cm^{-1}). As the excitation takes place locally in the phenol chromophore, which is weakly bound to the methanol moiety, this is a rather large effect on the methyl barrier. We performed ab initio calculations on methanol and on the species that might be responsible for this change of barrier height: the methoxonium cation as result of an intracluster proton transfer and the methoxonium radical as result of an intracluster hydrogen atom translocation upon electronic excitation. Only the latter species shows the observed reduction of the barrier height. Therefore, we assume the same hydrogen transfer in the excited state as in phenol–ammonia clusters to take place also in phenol–methanol clusters.

The phenol–water case is again similar to the phenol–ammonia case, although the conclusions are not so sound as in the other two cases. This is due to the fact, that the principal axis method (PAM) theory of internal rotors works strictly only for symmetric tops, attached to rigid frames, what is only approximately fulfilled for the water top. Nevertheless, since the hydrogen atoms are light the torsional axis changes its direction only slightly during rotation and the analysis in the PAM formalism still seems to be valid. From the reduction of the torsional constant upon electronic excitation, the translocation of the H atom from phenol can be assumed. This photoreaction has been recognized by Soboleski and Domcke as transition from the excited $^1\pi\pi^*$ state to the $^1\pi\sigma^*$ state[24] with a higher barrier than the respective transition in phenol–ammonia clusters. Jansen and Gerhards[41] showed that all six intermolecular modes are strongly coupled for the phenol–water complex. Thus, the strictly one-dimensional model applied herein might be not appropriate and the results for phenol–water clusters have to be regarded with more wariness.

To conclude, we found that in phenol clusters with ammonia, water, and methanol an H atom translocation in the first excited singlet state from phenol to the respective cluster partner takes place. Regarding the different nature (e.g., the acidities) of these substituents, H atom transfer in the excited state of phenol can be viewed as a quite general mechanism, already at the size of 1:1 clusters. The driving force for this excited-state hydrogen translocation is the nonadiabatic curve crossing between $^1\pi\pi^*$ states and $^1\pi\sigma^*$ states as has been postulated recently by Domcke and Sobolewski.[45] This curve crossing depends on the nature of the aromatic system and is supposed herein to lead to a higher barrier for excited-state hydrogen transfer in naphthol clusters than in the respective phenol clusters.

Further support of the interpretations given herein can be obtained from higher-level ab initio calculations of the excited states of these clusters. Structure optimizations for the systems discussed herein on the CASPT2 level for both electronic states involved in the transition are on the way and will be presented soon.

Acknowledgements

The financial support of the Deutsche Forschungsgemeinschaft (SCHM 1043/9-2 and 9-4) is gratefully acknowledged. We thank Prof. Karl Kleinermanns and Dr. W. Leo Meerts for stimulating discussions.

Keywords: computer chemistry · hydrogen transfer · internal rotation · isotope effects · vibrational spectroscopy

[1] J. D. Lewis, T. B. Malloy, Jr., T. H. Chao, J. Laane, *J. Mol. Struct.* **1972**, *12*, 427 – 449.
[2] C. C. Lin, J. D. Swalen, *Rev. Mod. Phys.* **1959**, *31*, 841 – 891.
[3] M. Blomberg, P. Siegbahn, *Mol. Phys.* **2001**, *101*, 323 – 333.
[4] G. Grégoire, C. Dedonder-Lardeux, C. Jouvet, S. Martrenchard, A. Peremans, D. Solgadi, *J. Phys. Chem. A* **2000**, *104*, 9087 – 9090.
[5] J. H. V. Vleck, *Rev. Mod. Phys.* **1951**, *23*, 213 – 227.
[6] W. Gordy, R. L. Cook, *Microwave Molecular Spectra, 3th Ed.*, Wiley, New York, **1984**.
[7] D. R. Herschbach, *J. Chem. Phys.* **1959**, *31*, 91 – 108.
[8] K. Levenberg, *Q. Appl. Math.* **1944**, *2*, 164 – 168.
[9] D. D. Marquardt, *J. Soc. Ind. Appl. Math.* **1963**, *11*, 431 – 441.
[10] X.-Q. Tan, W. A. Majewski, D. F. Plusquellic, D. W. Pratt, *J. Chem. Phys.* **1991**, *94*, 7721 – 7733.
[11] G. A. Bickel, G. W. Leach, D. R. Demmer, J. W. Hager, S. C. Wallace, *J. Chem. Phys.* **1988**, *88*, 1 – 8.
[12] T. M. Korter, D. W. Pratt, *J. Phys. Chem.B* **2001**, *105*, 4010 – 4017.
[13] D. M. Sammeth, S. S. Siewert, P. R. Callis, L. H. Spangler, *J. Phys. Chem.* **1992**, *96*, 5771 – 5778.
[14] K. Remmers, E. Jalviste, I. Mistrík, G. Berden, W. L. Meerts, *J. Chem. Phys.* **1998**, *108*, 8436 – 8445.
[15] D. Henseler, C. Tanner, H.-M. Frey, S. Leutwyler, *J. Chem. Phys.* **2001**, *115*, 4055 – 4069.
[16] S. J. Humphrey, D. W. Pratt, *J. Chem. Phys.* **1996**, *104*, 8332 – 8340.
[17] T. Droz, R. Knochenmuss, S. Leutwyler, *J. Chem. Phys.* **1990**, *93*, 4520 – 4532.
[18] D. Plusquellic, X.-Q. Tan, D. Pratt, *J. Chem. Phys.* **1992**, *96*, 8026 – 8036.
[19] A. Schiefke, C. Deusen, C. Jacoby, M. Gerhards, M. Schmitt, K. Kleinermanns, P. Hering, *J. Chem. Phys.* **1995**, *102*, 9197 – 9204.
[20] C. Jacoby, PhD thesis, Heinrich-Heine-Universität Düsseldorf, **1997**.
[21] G. Grégoire, C. Dedonder-Lardeux, C. Jouvet, S. Martrenchard, D. Solgadi, *J. Phys. Chem. A* **2001**, *105*, 5971 – 5976.
[22] V. Job, V. Patel, R. D'Cunha, V. Kartha, *J. Mol. Spectrosc.* **1983**, *101*, 48 – 60.
[23] R. Signorell, H. Palm, F. Merkt, *J. Chem. Phys.* **1997**, *106*, 6523 – 6533.
[24] A. L. Sobolewski, W. Domcke, *J. Phys. Chem. A* **2001**, *105*, 9275 – 9283.
[25] C. Plützer, C. Jacoby, M. Schmitt, *J. Phys. Chem. A* **2002**, *106*, 3998 – 4004.
[26] M. Schmitt, J. Küpper, D. Spangenberg, A. Westphal, *Chem. Phys.* **2000**, *254*, 349 – 361.
[27] A. Westphal, C. Jacoby, C. Ratzer, A. Reichelt, M. Schmitt, *Phys. Chem. Chem. Phys.* **2003**, *5*, 4114 – 4122.
[28] J. A. Hageman, R. Wehrens, de R. Gelder, W. L. Meerts, L. M. C. Buydens, *J. Chem. Phys.* **2000**, *113*, 7955 – 7962.
[29] W. L. Meerts, M. Schmitt, G. Groenenboom, *Can. J. Chem.*, in print.
[30] W. L. Meerts, M. Schmitt, unpublished results.
[31] F. J. Lovas, S. P. Belov, M. Y. Tretyakov, W. Stahl, R. D. Suenram, *J. Mol. Spectrosc.* **1995**, *170*, 478 – 492.
[32] M. C. L. Gerry, R. M. Lees, G. Winnewisser, *J. Mol. Spectrosc.* **1976**, *61*, 231.
[33] T. Anderson, F. C. Lovas, *Ap. J. Suppl.* **1990**, *72*, 797 – 814.
[34] G. Berden, W. L. Meerts, M. Schmitt, K. Kleinermanns, *J. Chem. Phys.* **1996**, *104*, 972 – 982.
[35] M. Schmitt, C. Jacoby, K. Kleinermanns, *J. Chem. Phys.* **1998**, *108*, 4486 – 4495.
[36] W. Roth, PhD thesis, Heinrich-Heine-Universität Düsseldorf, **1998**.
[37] W. S. Benedict, N. Gailar, E. K. Plyler, *J. Chem. Phys.* **1956**, *24*, 1139 – 1165.
[38] F. Chen, E. R. Davidson, *J. Phys. Chem. A* **2001**, *105*, 10915 – 10921.
[39] M. Schütz, T. Bürgi, S. Leutwyler, T. Fischer, *J. Chem. Phys.* **1993**, *98*, 3763 – 3776.
[40] S. Melandri, A. Maris, P. G. Favero, W. Caminati, *Chem. Phys.* **2002**, *283*, 185 – 192.
[41] A. Jansen, M. Gerhards, *J. Chem. Phys.* **2004**, *121*, 1271 – 1277.
[42] T. Ebata, A. Fujii, N. Mikami, *Int. J. Mass Spectrom. Ion Processes* **1996**, *159*, 111 – 124.
[43] T. Ebata, N. Mizuochi, T. Watanabe, N. Mikami, *J. Phys. Chem.* **1996**, *100*, 546 – 550.
[44] D. Feller, M. W. Feyereisen, *J. Comput. Chem.* **1993**, *14*, 1027 – 1035.
[45] W. Domcke, A. L. Sobolewski, *Science* **2003**, *302*, 1693 – 1694.

Received: June 15, 2004

